Experimental Analysis and Modeling of the Crack Arrest Condition Under Severe Plastic Fretting Fatigue Conditions

Camille Gandiolle, Siegfried Fouvry

Available online at www.sciencedirect.com

SciVerse ScienceDirect

Procedia Engineering 00 (2013) 000–000

Procedia Engineering

www.elsevier.com/locate/procedia

5th Fatigue Design Conference, Fatigue Design 2013

Experimental analysis and modeling of the crack arrest condition under severe plastic Fretting Fatigue conditions

Camille Gandiolle[a]*, Siegfried Fouvry[a]

[a)]*LTDS, Ecole Centrale de Lyon, 36 avenue Guy de Collongue, 69134 Ecully Cedex, France*

Abstract

The fretting-fatigue crack arrest condition is formalized as the condition for which a crack nucleates but stops propagating and so the sample never fails. Usually this domain is small as the fatigue loading greatly promotes the crack propagation. The aim of this research work is to investigate the crack arrest condition for severe plastic condition (maximal pressure is 2.5 times greater than the yield stress) and high fatigue stress ratio (R=0.94) thus for not much propagating conditions.
A low alloyed industrial steel flat specimen (IS) fretted against a 35NCD16 steel cylinder pad was studied in order to identify the crack arrest condition for various fretting loadings (shear amplitude). An original experimental monitoring has been implemented on a fretting-fatigue test device to observe on-line the crack arrest using the potential drop technic. To rationalize these results, a fretting-fatigue map concept which consists to plot the crack arrest boundary as a function of the applied maximum fatigue stress and the fretting tangential force amplitude is applied [1].
A 2D plain strain FEM modelling has been implemented to simulate the complex contact stressing including the contact plasticity. This plastic deformation promotes a significant extension of the contact and a proportional reduction of contact pressure and cyclic shear stresses. One consequence is that for a given contact and fatigue loading, this plastic accommodation of the interface tends to reduce the effective stress imposed to the material.
The crack arrest boundary was formalized applying a pure mode I effective intensity stress range approximation [2]. It is shown that combining elastic-plastic FEM modelling, weight function and an adequate estimation of the effective intensity stress range, it is possible to predict with accuracy the fretting fatigue crack arrest boundary.

Selection and peer-review under responsibility of CETIM, Direction de l'Agence de Programme.

Keywords: fretting-fatigue; elastic-plastic modelling; crack arrest; K-factor

* Corresponding author. Tel.: +33-047-218-6044; fax: +33-047-833-1140.
E-mail address: camille.gandiolle@gmail.com

Selection and peer-review under responsibility of CETIM, Direction de l'Agence de Programme.

1. Introduction

Fretting is defined as a small oscillatory movement between two bodies in contact which induce relative displacement between the two surfaces. Combined with cyclic bulk fatigue loading, the so called fretting-fatigue loading can induce catastrophic damages such as wear or cracking, which critically reduce the endurance of assemblies. This study concentrates on cracking damage and is thus restricted to the partial slip domain. Below a threshold fretting fatigue condition, no crack is nucleated and the system runs under safe crack nucleation condition. Above this threshold, a crack will nucleate but not necessarily propagate. Imposing higher stress condition leads to crack propagation until failure is reached (Fig. 1a).

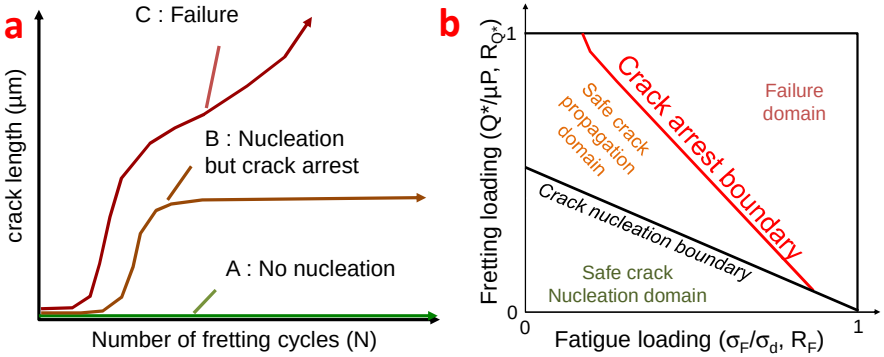

Fig. 1. (a) Crack nucleation and propagation in fretting-fatigue; (b) Fretting fatigue map.

A significant effort has been made during the past decade both to formalize the crack nucleation and the crack arrest conditions. To rationalize the prediction of cracking risk induced by fretting-fatigue, a fretting-fatigue map concept which consists to plot the crack nucleation boundary and the crack arrest boundary as a function of the applied maximum fatigue stress (x-axis) and the fretting tangential force amplitude (y-axis) has been introduced [1] (Fig. 1b). Like for any fatigue problem, the mean stress level plays a critical role in the damage evolution. The mapping description is thus relevant only for R_F and R_{Q*}, the fatigue and fretting stress ratios, and a given contact configuration.

This work focuses on the crack arrest. The literature suggests that the crack will arrest if the effective stress intensity range ΔK_{eff} falls below a threshold value ΔK_{th} [3,4]. The crack arrest condition allows plotting a crack arrest boundary which delimits a safe design area despite the presence of cracks. First we will present the experimental results and discuss them. Then the crack arrest description will be formalized by computing the evolution of the stress intensity factor below the surface taking the plasticity into account. Then the crack arrest is predicted by means of a threshold value calibrated on plain fretting test.

2. Materials and tests

Table 1. Mechanical properties of the tested materials.

Materials	35NCD16	Industrial steel (IS)
Young's modulus E (GPa)	210	190
Poisson's ratio ν	0.3	0.29
Yield stress σ_Y (0.2%) (MPa)	1127	σ_Y
Ultimate stress σ_{UTS} (MPa)	1270	σ_{UTS}

The fretting-fatigue crack arrest response of a low alloyed industrial steel (IS) will be investigated using a cylinder/plane configuration. The cylinder pad consists of a tempered 35NCD16 steel with a cylinder radius of R=19mm and a lateral width of L=10mm. Their mechanical properties are presented in Table 1. IS properties are confidential but it is considered homogeneous and it is described by a monotonic elastic-plastic law determined by

simple tensile test.

The contact is tested in plain fretting and fretting-fatigue. Both test principle are sketched in Fig. 2. In both case, a high static normal force P is applied so that severe plastic deformations are induced in the flat: $p_0/\sigma_y = 2.5$ (p_0 maximum pressure in the flat). The fatigue and fretting stress ratios are kept constant at respectively $R_F = 0.94$ and $R_{Q^*} = -1$. The crack analysis is restricted to the IS steel flat specimen. The dimensions chosen allow plain strain conditions along the central axis of the fretting scar. All the fretting scars were analyzed following a method developed by Proudhon et al. [5]. The main steps of this method are explained in the following part.

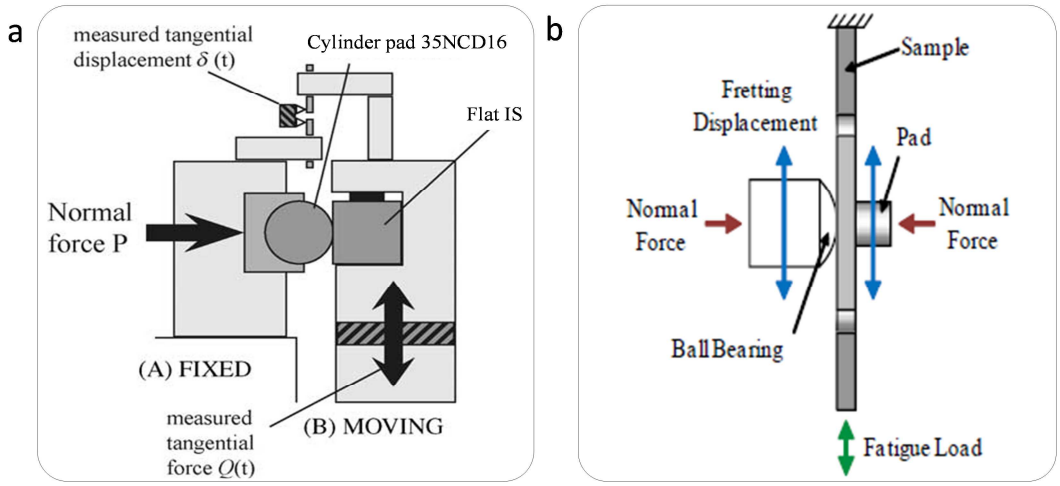

Fig. 2. (a) Plain fretting test; (b) Fretting-fatigue test.

3. Experimental identification of the crack arrest

3.1. Fretting fatigue crack arrest: destructive analysis

Crack arrest is defined as the condition for which a crack is nucleated but stop propagating after a time due to the very sharp decrease of the contact stress influence below the interface. For high propagating conditions such as low fatigue stress ratios ($R_F = -1$ or $R_F = 0.1$) the crack arrest condition is easily obtained by destructive test: indeed the crack propagation is so fast that the failure time can be considered as the end of the crack arrest condition. However in this work, a really high fatigue ratio is studied: $R_F = 0.94$. Consequently, the crack propagates very slowly and it would imply too long tests to establish the crack arrest condition. Alternative strategies are considered.

A first option was to stop the same test after various numbers of fretting cycles and observe the evolution of the crack length. As presented in Fig. 3a, the studied sample is cut in the middle, then imbed in epoxy to be polished to a mirror surface state. Next the cracks are observed with an optical microscope. For each experimental test, the maximum projected crack length is considered and plotted as a function of the number of fretting-fatigue cycles. The loads applied correspond to a crack arrest condition if the crack stops growing: if it shows a plateau as a function of the number of fretting-fatigue cycles as plotted in the example Fig. 3b. However this method is very time consuming as it requires several tests to establish if the crack arrest condition is effectively reached. Furthermore the evaluating technique is destructive and time consuming too as three different cross sections observations need at least to be considered to correctly estimate the maximum crack length generated along the fretting scars. So a second option has been investigated: the potential drop technique.

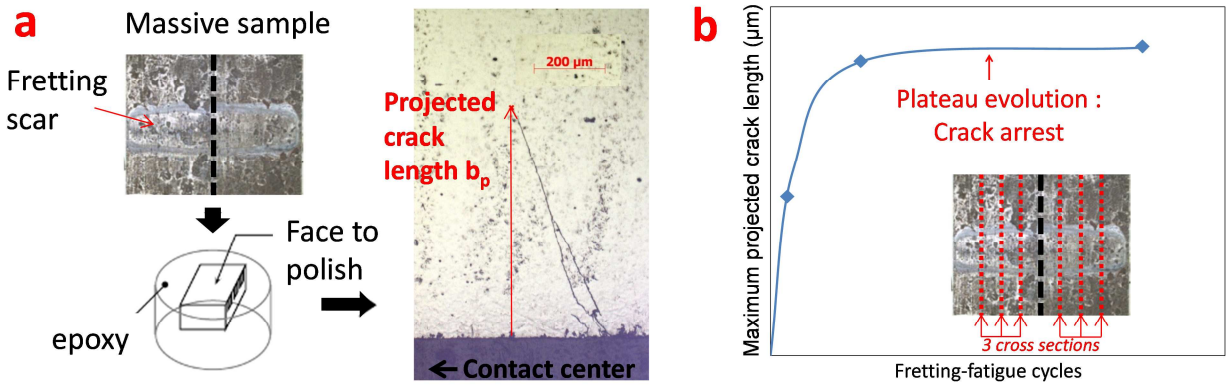

Fig. 3. (a) Optical analysis method (b) Experimental fretting-fatigue crack arrest condition

3.2. Potential drop technique (PDT): online analysis of the crack propagation

The potential drop technique (PDT) is a well-known technique to observe crack propagation in fatigue test. The practice was first introduced in 1957 by Barnett and Troiono [6]. The technique has been widely used and the calibration procedure is well known [7]. The idea of applying the PDT on a fretting fatigue device was first introduced by Kondo et al. [8]. It was first implemented on a fretting-fatigue test in the LTDS by Mériaux [9]. This technique relies on the fact that the potential distribution in the vicinity of a crack changes with crack growth. Fig. 4 shows photography and a sketch of the set up.

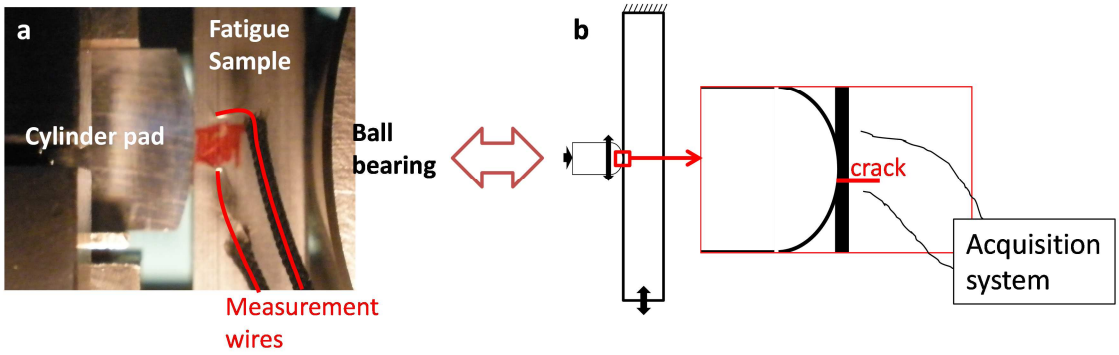

Fig. 4. (a) Photo of the contact with the measurement wires; (b) PDT set up.

A current is applied through the fatigue test sample. Platinum wires are welded on the sample surface on each side of the contact (2 wires per surface) and on both side of the sample (4 wires in total). On each surface, a potential is measured between the two wires with the acquisition system. The potential measured depends on the sample resistance. When a crack nucleates and propagates, the sample cross section diminishes and thus the electrical resistance increases. With the acquisition system, a variation of the potential measured is hence observed. By measuring the potential on each side of the sample and taking the mean value of the potential, the possible non homogeneity of the crack propagation in the sample is account for. This method allows for direct information on the crack propagation, so only one nondestructive test is necessary to know if a loading condition is a crack arrest condition.

3.3. Experimental application of the PDT

The potential drop technique was applied on the fretting-fatigue test. Three different behaviors have been observed. On one hand, as shown in Fig. 5a, the normalized potential increases, indicating that a crack exists and propagates. Then the potential stabilizes to a very low slope $K_e<10^{-9}$ which suggests that the crack arrest condition is

reached. On the other hand, as shown in Fig. 5b, the potential ratio may continuously increase all test long with a slope $K_e > 10^{-9}$. This situation was related to a crack propagation condition. Finally there may be failure as shown in Fig. 5c. From these behaviors, a criterion is established: if $K_e<10^{-9}$, there is crack arrest, if $K_e>10^{-9}$ there is no crack arrest.

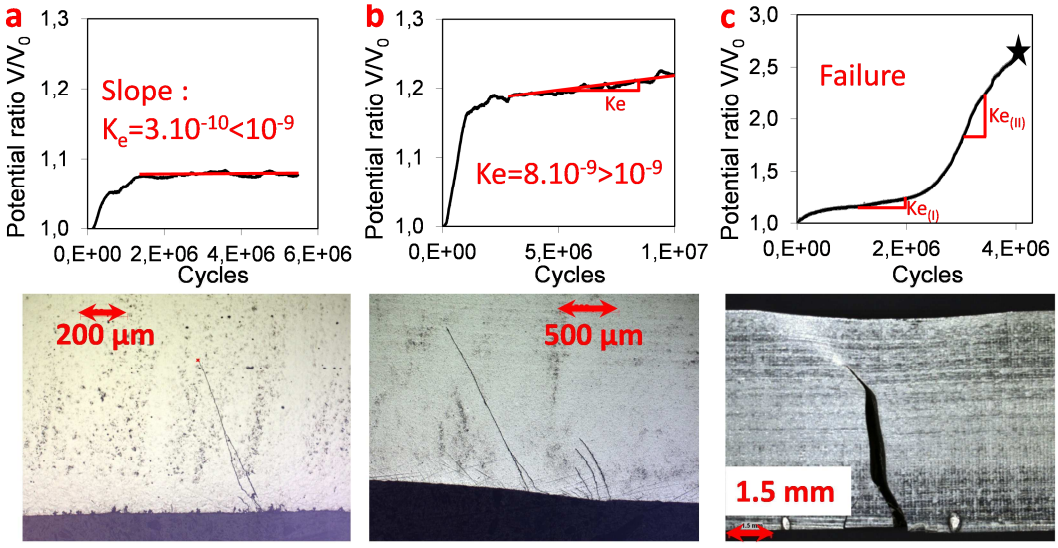

Fig. 5. (a) Crack arrest condition; (b) Crack propagation condition; (c) Failure condition. V_0: potential measured at the test beginning

With this consideration, the potential drop technique was systematically applied for all the experimental fretting fatigue analysis. The tests were all stopped after 10^7 fretting-fatigue cycle if the crack arrest condition or the failure was not reach before. Fig. 6 plots the experimental crack arrest fretting-fatigue map obtained with the potential drop technique. Along each point the crack lengths at the end of the test are given. For $K_e>10^{-9}$, it corresponds to the crack obtained after 10^7 cycles, but if the test was let running, it would increase until failure.

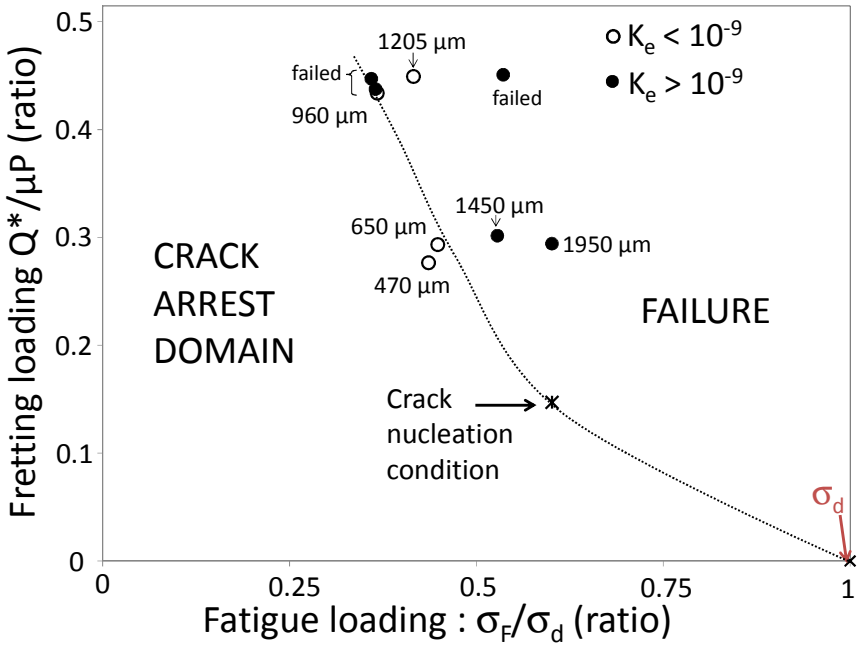

Fig. 6. Crack arrest experimental fretting-fatigue map

This analysis suggests that it is possible to reach the crack arrest condition even for really long cracks. From these points the crack arrest boundary is plotted as a function of the fretting and fatigue loadings (Fig. 6).

4. Prediction of the crack arrest condition

4.1. FEM modeling

Finite element analysis (FE) was carried out using Abaqus 6.9. Two dimensional plane strain modelling of the fretting fatigue test has been generated following the sketch shown in Fig. 7. The dimensions are conformed to the experimental test. The ball bearing is assumed to have no impact on the sample stress field therefore a symmetric condition is used with a significant width. The model is meshed with linear triangle elements types CPE3 except in the contact zone where linear quadrilateral elements types CPE4R have been used. In addition, this zone is meshed more densely than the other regions (5 µm long squares).

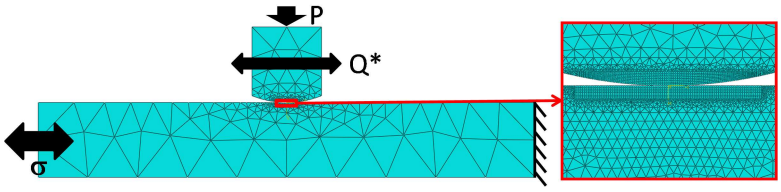

Fig. 7. Abaqus model of the test.

A surface to surface discretization with small sliding is adopted for contact accommodation. The Lagrange multiplier with the friction coefficient f=0.8 was selected as the contact algorithm. The constraints, displacements and loads applied reproduce exactly the experimental test. The cylinder is elastic and its properties are given in Tab. 1. The flat is described with a monotonic elastic-plastic law. As a consequence, the normal force and then the fretting-fatigue cycles create plasticity in the contact. The amount of plasticity decreases after each cycle due to the material hardening but above all to the contact geometry plastic accommodation. The evolution of the equivalent plastic strain at integrations points with the cycle number is thus observed (Fig. 8). When an asymptotic condition is attained, the elastic shakedown has been reached. A numerical analysis shows that the elastic shakedown is achieved after at least 75 loading cycles. When the contact stabilizes, the stress loading $\underline{\Sigma}(t)$ of the last cycle is considered to compute the stress intensity range thus to formalize the crack arrest condition.

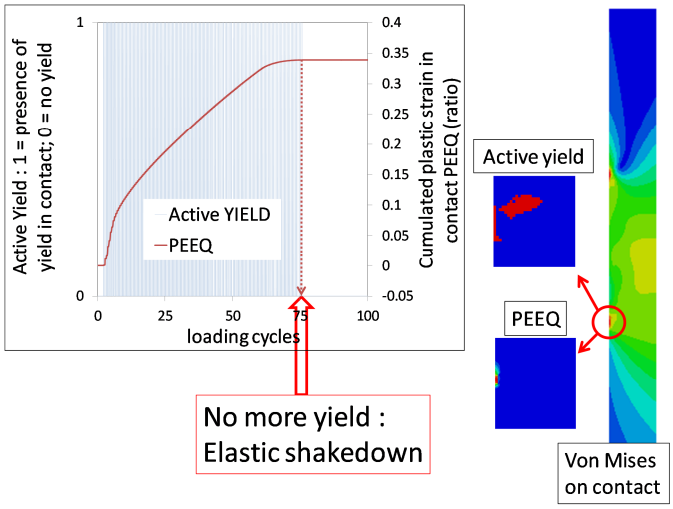

Fig.8. Monitoring of the elastic shakedown on contact.

4.2. Influence of plasticity

The fretting fatigue experimental crack arrest condition (σ_F/σ_d=0.435, Q*/μP=0.294) is computed to observe the influence of the severe plastic conditions imposed by the experimental test conditions. Two computations hypothesis were considered. The first one assumes a full elastic response of both plane and cylinder specimens, and a second one, more representative of the experimental analysis, considers an elastic response of the cylinder but an elastic-plastic (EP) response of the plane equivalent to the monotonic stress-strain behaviour of the IS steel. Fig. 9a plots the contact pressure and shear obtained after the elastic shakedown.

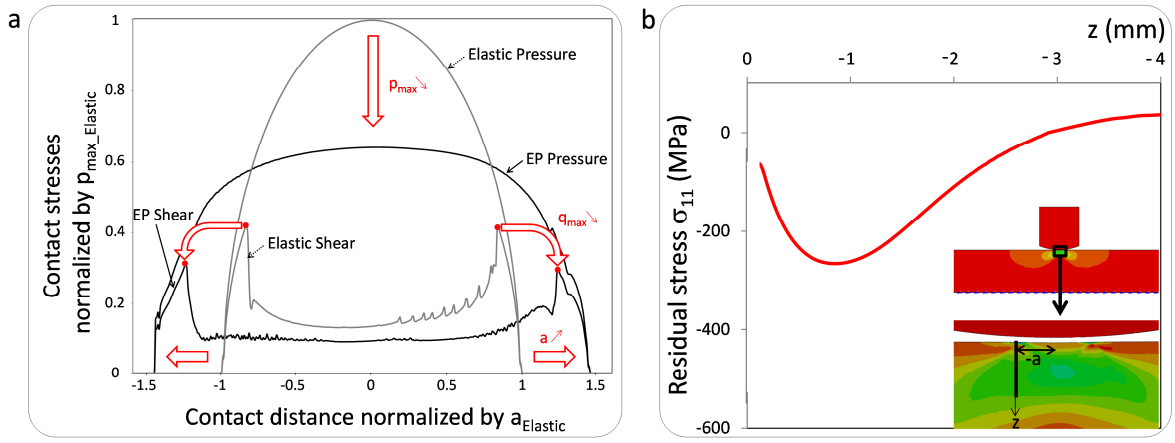

Fig. 9. (a) Contact stresses; (b) Distribution of the σ_{11} residual stress (after the contact opening) (σ_F/σ_d = 0.435, Q*/μP =0.294)

The plastic strain in the contact leads to a reduction of the maximum contact pressure $\boldsymbol{p_{max}}$, and of the maximum shear stress $\boldsymbol{q_{max}}$ as the same time as the contact radius $\boldsymbol{a}$ increases. This plastic accommodation highly modifies the subsurface stressing which suggests that an EP analysis is required to model the crack propagation process.
Besides, the σ_{11} residual stresses generated below the surface at the trailing contact border (x=-a) are significant and compressive (Fig. 9b). They diminish and get closer to zero only below 3 mm. The very severe plastic conditions imposed generate large contact plastic accommodations and strong compressive residual stresses that may only be addressed applying an elastic-plastic modelling.

4.3. Prediction methodology

The crack arrest description is formalized by computing the evolution of the stress intensity factor below the surface taking the plasticity into account as described before. First the studied condition is computed using the model presented in 4.1, then the normal stressing along the expected crack path are extracted at the contact border for the maximum and minimum loading conditions as schematized in Fig. 10.

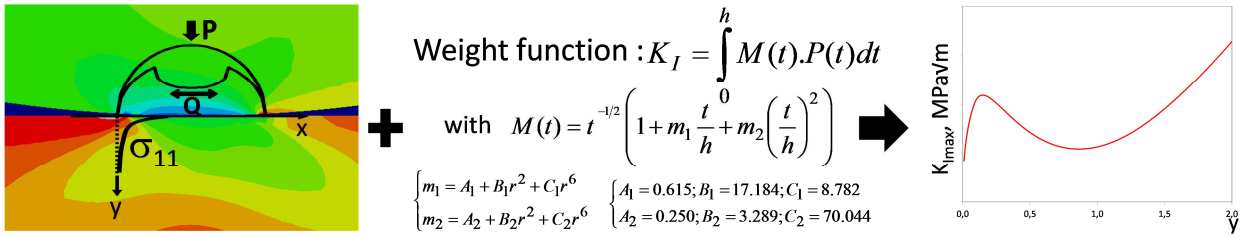

Fig. 10. Stress extraction along crack path for a fretting fatigue case.

From those stressing, the maximum K_{1max} and minimum K_{1min} stress intensity factor are calculated using a common weight function approach (Fig. 10). This function calculates the K-factor from the finite element computed stress state below the contact. Finally, the effective stress intensity range ΔK_{eff} along the crack path is determined using

the Elber approximation thus to consider the crack closure effect induced by compressive conditions (negative R_K):

- For $R_K>0$; $\Delta K_{eff} = K_{1max}-4$
- For $-1<R_K<0$; $\Delta K_{eff} = K_{1max}-(4.R_K+4)$ with $R_K = K_{Imin}/K_{Imax}$
- For $R_K<-1$; $\Delta K_{eff} = K_{1max}$

The mode II contribution is neglected [2] and only the elastic-plastic analysis is considered here.

4.4. Subsurface stresses study

For the above condition ($\sigma_F/\sigma_d=0.435$, $Q^*/\mu P=0.294$), the principal stress $\sigma_{11,min}$ and $\sigma_{11,max}$ are extracted at the contact border and plotted in Fig. 11a as a function of the distance to the surface. It shows that after a given depth (here 2 mm), both stresses join each other meaning this distance is out of the contact influence zone.

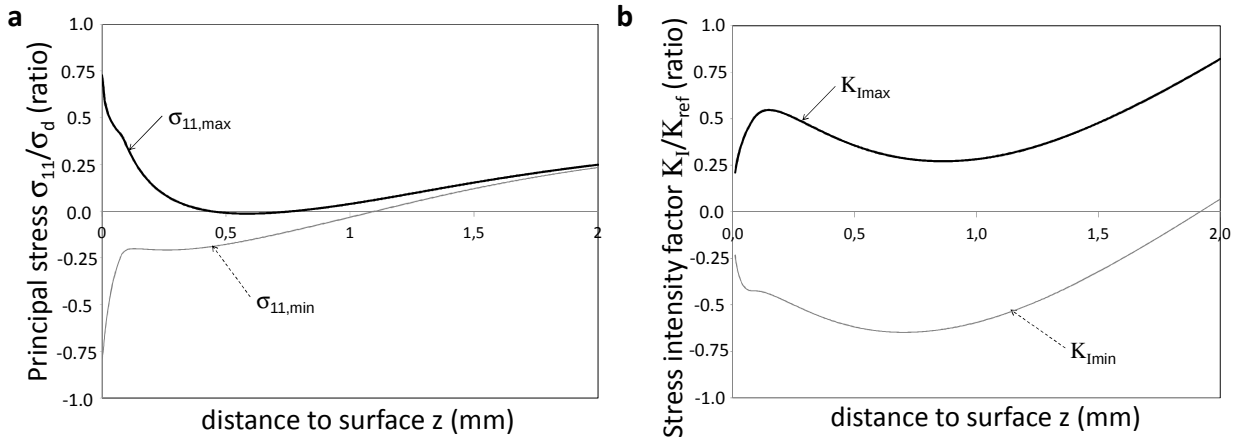

Fig. 11. (a) Principal stress at the contact border; (b) Stress intensity factors at the contact border

With the weight function, the maximum and minimum stress intensity factors K_{Imax} and K_{Imin} are calculated and plotted in Fig. 11b. K_{Imin} is almost always negative in the domain studied: from the surface to 2 mm below. So when the R_K factor is plotted as a function of the distance to surface in Fig. 12a, there is a large zone where the ratio is inferior to 1. Coincidently, looking at the experimental crack length studied in Fig. 6, it corresponds to the crack arrest domain. So, in the crack arrest conditions domains, despite the really high fatigue stress ratio studied $R_F=0.94$, R_K remains inferior to -1 and thus $\Delta K_{eff} = K_{Imax}$. This confirms the observations of Nowell and Dini [2]. It was however chosen to continue using the Elber approximation for all effective intensity stress range determination to remain conservative.

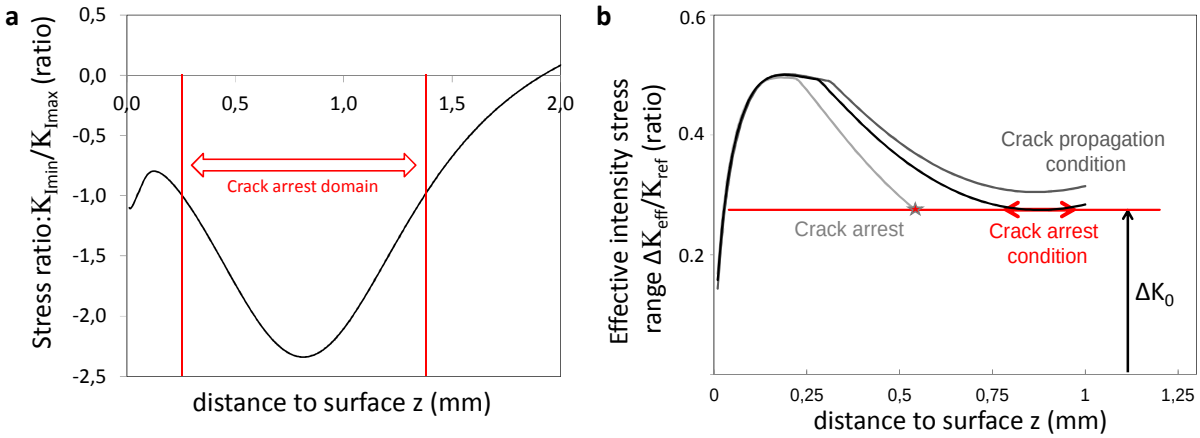

Fig. 12. (a) R_k stress ratio along the crack path; (b) crack arrest condition determination.

The calculated stress ranges are plotted as a function of the distance to the surface. A stress condition is considered in crack arrest when the computed effective stress intensity range along the expected crack path crosses a crack arrest condition. When the effective stress intensity range doesn't cross the crack arrest condition, the crack propagates until failure. The crack arrest condition is reached when the effective stress intensity factor range reaches tangentially the crack arrest limit. As the short crack domain is estimated below 50 µm, the studied crack arrest conditions are assumed in the long crack regime. The crack arrest condition is therefore related to a constant ΔK_0 value as schematized in Fig. 12b. The discontinuity of the curves comes from the evolution of the stress ratio R_K below the interface, leading to different Elber approximation of ΔK_{eff}.

5. Reverse identification of ΔK_0 from plain fretting cracking analysis

The given crack arrest prediction strategy requires knowing the long crack threshold value ΔK_0. Unfortunately this value was not established for the studied IS alloy. Therefore, an original reverse strategy was applied. It consists in estimating the ΔK_0 value by modelling the crack arrest conditions related to plain fretting cracking conditions. Indeed, in plain fretting, because no external fatigue stressing is imposed, the crack arrest condition is systematically reached after 10^6 cycles.

An additional plain fretting cracking analysis has been performed for similar contact geometry and normal loading but for varying applied tangential force amplitude. This is to estimate the evolution of the maximum crack length reached at the crack arrest condition after 10^6 partial slip cycles (Fig. 13a).

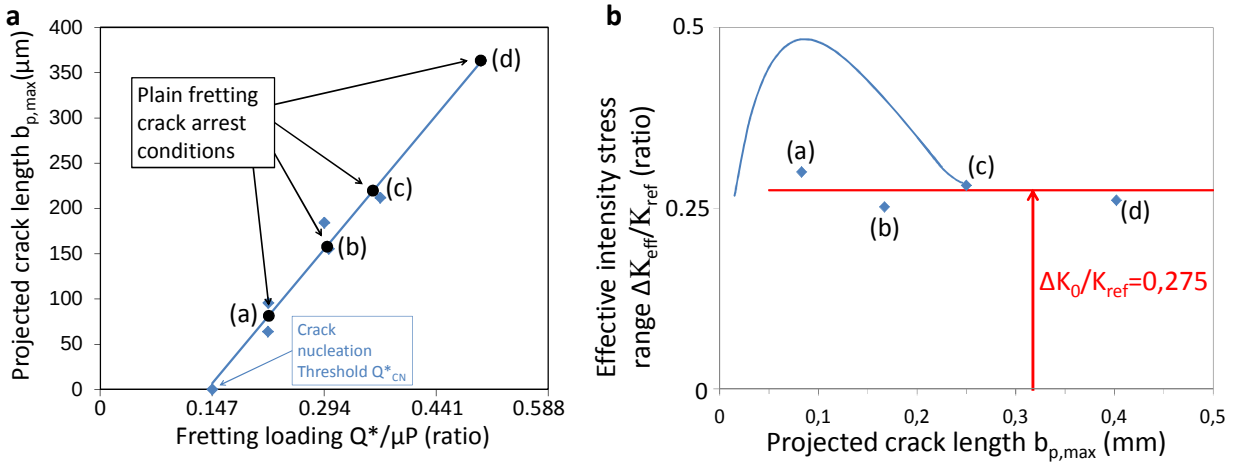

Fig. 13. (a) Plain fretting experimental results; (b) Crack arrest condition identification on plain fretting conditions (P, 10^6 cycles, 12 Hz)

The tests were simulated and their effective stress intensity ranges are calculated along their expected crack path as explained before. The crack tip effective stress intensity range are extracted and plotted in Fig. 13b as a function of the crack tip depths. A constant evolution is observed which allows extrapolating the long crack threshold value $\Delta K_0/\Delta K_{ref}$=0.275. The theoretical crack arrest boundary defined from the monotonic elastic-plastic law can now be computed. For a constant tangential load, several fatigue stressing are computed. The crack arrest condition is reached when the effective intensity stress range reaches tangentially the crack arrest limit as described before. Fig. 14 plots the obtained crack arrest boundary. The computed fretting fatigue crack arrest limit is very close to the experimental results and moreover provides a slightly conservative estimation of the crack arrest domain.

This confirms the stability of the proposed methodology where the fretting fatigue crack arrest condition can be predicted applying an elastic-plastic analysis of the contact stress field, coupled with an adequate estimation of the stress intensity factor range and where the threshold ΔK_0 crack arrest value is established from a reverse analysis of well-established plain fretting crack arrest conditions.

Besides, in addition to estimate the ΔK_0 parameter, the plain fretting crack analysis allows us to estimate a second crack nucleation condition when no external fatigue stressing is imposed so that the fretting fatigue crack nucleation boundary can be approximated (Fig. 14).

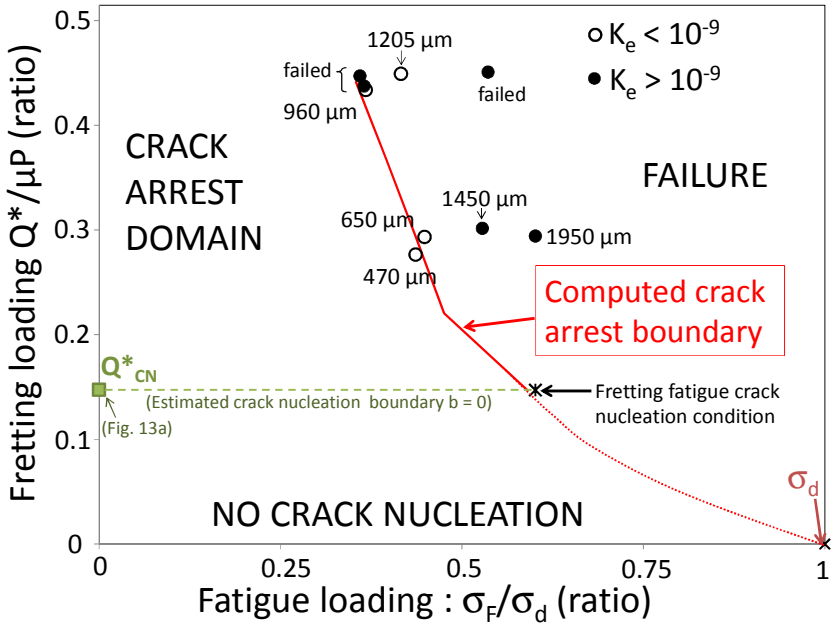

Fig. 14. Computed crack arrest fretting fatigue map.

6. Conclusion

The crack arrest in steel/steel contact was observed for severely plastic conditions and a high fatigue stress ratio. The low crack propagation induced by the high fatigue ratio has been resolved experimentally by using a fast online method: the potential drop technique. In addition an experimental crack arrest criterion has been defined: for $K_e<10^{-9}$, there is no crack propagation but for $K_e>10^{-9}$, the crack propagates. Using this fast methodology the experimental fretting fatigue crack arrest boundary was defined (Fig. 6).

This boundary has been successfully predicted by means of an innovative decoupled approach: the contact stress state is obtained by elastic-plastic FEM modelling, then the stress intensity factors are calculated with a weight function and finally the Elber approximation is used to obtain the effective stress intensity range along the crack.

To determine the ΔK_0 parameter required by the model, an original inverse analysis of well-established plain fretting crack arrest conditions was applied. This approach displayed very stable and conveniently conservative predictions. Beside we demonstrated that most of the crack arrest conditions were achieved for crack lengths where the R_K ratio is always inferior to -1 so that the common $\Delta K_{eff}= K_{Imax}$ approximation is justified [2].

Future work needs now to better define the transition from crack arrest to crack nucleation boundary and needs coupling a more representative cyclic plastic law.

References

[1] K. Kubiak, S. Fouvry, a. M. Marechal, A practical methodology to select fretting palliatives: Application to shot peening, hard chromium and WC-Co coatings, Wear. 259 (2005) 367–376.

[2] D. Dini, D. Nowell, I.N. Dyson, The use of notch and short crack approaches to fretting fatigue threshold prediction: Theory and experimental validation, Tribology International. 39 (2006) 1158–1165.

[3] H. Kitagawa, S. Takahashi, Application of fracture mechanics to very small cracks or the cracks in the early stage, American Society for Metals. (1976) 627–630.

[4] T.T.H. Haddad El M. H., Smith K. N., Fatigue crack propagation of short cracks, Jurnal of Engeneering Materials and Technology. 101 (1979) 42–46.

[5] H. Proudhon, S. Fouvry, G.R. Yantio, Determination and prediction of the fretting crack initiation : introduction of the (P , Q , N) representation and definition of a variable process volume, i (2006) 707–713.

[6] W. Barnett, A. Troiono, Crack Propagation in Hydrogen Induced Brittle Fracture of Stee, J Met. 9 (1952) 94.

[7] H. Johnson, Calibrating the electric potential method for studying slow crack growth, Mater Res Stand. 5 (1965) 5.

[8] Y. Kondo, C. Sakae, M. Kubota, K. Yanagihara, Non-propagating crack behaviour at giga-cycle fretting fatigue limit, Fatigue Fracture of Engineering Materials and Structures. 28 (2005) 501–506.

[9] J. Meriaux, S. Fouvry, K. Kubiak, S. Deyber, Characterization of crack nucleation in TA6V under fretting–fatigue loading using the potential drop technique, International Journal of Fatigue. 32 (2010) 1658–1668.